Correlations in Prime Number Distribution and L-function Zeros

O. Shanker

Hewlett Packard Company, 16399 W Bernardo Dr., San Diego, CA 92130, U. S. A.
oshanker@gmail.com
http://<www.geocities.com/oshanker/primedistribution.htm>

A simple analysis of the gaps in primes shows an interesting correlation between neighbouring primes. Neighbouring primes are more likely to have differing remainders on being divided by 6 (the remainders can be 1 or 5). We give a heuristic argument for the observed correaltion. We apply the tool of rescaled range analysis to study the statistical properties.

Keywords: Distribution of Primes; Zeta Functions; Fractals;
(updated Apr. 8, 2009)

1. Introduction

We report an interesting correlation between neighbouring primes uncovered during an analysis of the prime number gaps. While the distribution of prime number gaps has been studied extensively, the particular correlation reported here doesn't seem to have been documented.

Section 2 analyses the distribution of prime numbers, and finds that neighbouring primes are more likely to have differing remainders on being divided by 6 (the remainders can be 1 or 5). A heuristic model is presented to explain the correlation, and the need for further investigation is pointed out. Section 3 applies rescaled range analysis to the prime number gaps. Sections 4 and 5 apply it to the zeros of the L-functions. Finally the conclusions are presented, followed by an appendix which considers the rescaled range analysis for zeros of the Hermite Polynomials.

2. Distribution of Prime Numbers

We study the statistical properties of the distribution of prime number gaps. Earlier studies of the gaps give detailed information on the asymptotic behaviour of the distribution [1,2,3,4,5,6,7,8]. A strong form of the k-tuple conjecture [9] leads to an explicit asymptotic formula for the frequency with which an integer D appears as the difference of consecutive primes $\leq x$. Brent [4] was the first to suggest this formula and gave an algorithm for computing certain coefficients that arise in the formula. In this paper we present numerical evidence and a heuristic model for a correlation between neighbouring primes. These results provide information about the statistical properties of the prime number gap distribution which is additional to that provided by the quantitative form of the k-tuple conjecture.

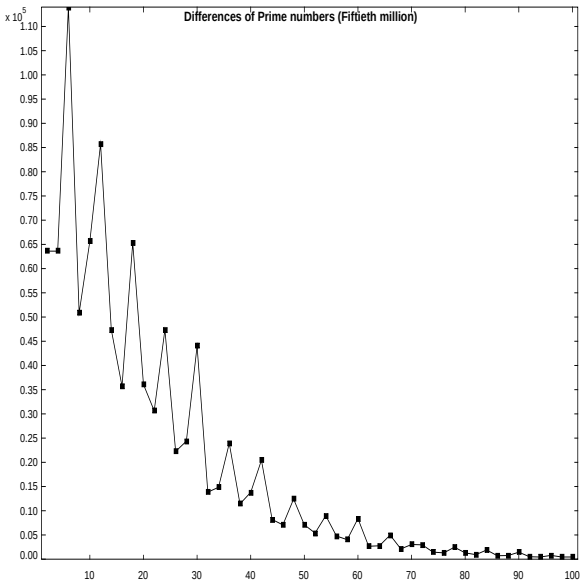

Fig. 1. Histogram of prime number differences for fiftieth million set of primes. The y axis is the frequency and the x axis is the difference between neighbouring primes.

Figure 1 shows the histogram of the prime number differences for the fitftieth million set of primes. We observe that the histogram shows structure. The peaks at differences which are multiples of 6 is the most obvious feature, and is easily explained by the fact that when a prime number is divided by 6, the remainder is either 1 or 5. However, what is interesting and new in the results presented here is that an analysis of the peaks shows correlations between the probability of the remainder being 1 or 5 for a particular prime number and the remainder for the next prime number. From the histogram we get the following probabilities:

$$Prob(diff = 6k + 2) = Prob(diff = 6k + 4) = .276; \quad (1)$$

$$Prob(diff = 6k) = 0.448; \quad (2)$$

If there were no correlations between neighbouring primes, then the values would be

$$Prob(diff = 6k + 2) = Prob(diff = 6k + 4) = .25; \quad (3)$$

$$Prob(diff = 6k) = 0.50; \quad (4)$$

We find that the probabilities for neighbouring primes are correlated. Table 1 shows the joint probabilities between the remainder for a given prime on division by 6 and the remainder for the next prime, for the fiftieth million set of primes $(961748941 \ldots 982451653)$ and the tenth million set of primes$(160481219 \ldots 179424673)$ [10]. The remainders for the first prime are shown

in the rows, while the remainder for the second prime are shown in the columns. Note that the remainder for the next prime has a higher likelihood of being different from the first remainder. We see that the ratio of the number of neighbouring primes with the same remainder to the number of neighbouring primes with different remainders is 0.811 for the fiftieth million set of primes. Further evidence of this striking result comes from Table 2 which shows the correlations on division by 4 (which can give the remainders 1 and 3) .

One can give a heuristic argument for the correlation. All primes will be of the type $6k+1$ or $6k+5$. These two arithmetic progressions are interlaced. We know that the density of primes at N is of order $1/ln(N)$. Let us consider a heuristic model, i.e., each term in either of the arithmetic progressions has a "probability" $3/ln(N)$ of being prime. The heuristic model predicts that the the ratio of the number of neighbouring prime pairs with the same remainders to the number of neighbouring prime pairs with different remainders is $(1-3/ln(N))$, which numerically is 0.85 for the fiftieth million set of primes, almost the observed value. While the heuristic model is quite interesting, it is not a rigorous proof for the correlation. Further, it cannot be the complete story, since it predicts that the a gap of 6 will be the most likely gap, while the work on jumping champions [1] (an integer D is called a jumping champion if D is the most frequently occurring difference between consecutive primes $\leq x$ for some x) shows that for very large numbers the most likely gap will be a primorial larger than 6. Thus, the correlation reported here and the heuristic explanation point to areas that ought to be investigated further.

3. Rescaled Range Analysis

An useful tool for studying correlation in series is rescaled range analysis. An analysis of the zeros of the Riemann zeta function using rescaled range analysis [11] gave some remarkable results. The differences of the zeros were found to have a strong anti-correlation, implying a large fractal dimension for the zero distribution. In this section we give a brief review of rescaled range analysis and apply it to the prime number gaps. In the next section we apply it to degree 1 and degree 2 L functions.

Rescaled range analysis [12,13,14,15] is a tool to study series of observations which exhibit a combination of random or pseudo-random behaviour and regular behaviour. In particular, it shows whether the successive observations of the variable under study are correlated or independent. It is based on the process of fractional Brownian motion. A time series observable X(t) is said to undergo fractional Brownian motion of order α if $X(t)$ has the properties:

(1) With probability 1 $X(t)$ is a continuous function of t which is nowhere differentiable.
(2) For any $t \geq 0$ and $h > 0$, the increment $X(t+h) - X(t)$ is normally distributed with mean 0 and variance proportional to $h^{2\alpha}$. With suitable normalisation,

$$Prob(X(t+h) - X(t) \leq x) = (2\pi)^{-1/2} h^{-\alpha} \int_{-\infty}^{x} exp(-u^2/2h^{2\alpha}) du. \quad (5)$$

The increments $X(t+h)-X(t)$ and $X(t)-X(t-h)$ are not independent unless α is 1/2. If $\alpha > 1/2$ then the increments tend to be of the same sign. $\alpha = 1/2$ is the case of normal Brownian motion. If $\alpha < 1/2$ then the increments tend to differ in sign. α is called the Hurst exponent. With probability 1 $X(t)$ has Hausdorff dimension and box dimension both equal to $2-\alpha$. Rescaled range analysis makes use of Eqn. 5 and determines the order of the fractional Brownian motion by studying how the vertical range X scales with the horizontal range h. It has been applied to fluctuations in the stock market, financial analysis, analysis of annual variations in river flood levels, study of the zero distribution of the Riemann zeta function, etc.

We denote the series of increments ocurring in the rescaled range analysis by δ_j. Rescaled range analysis studies the correlations of the δ_j by boxing the observed data into bins of different sizes (the bin size being denoted by h), and by studying how the vertical range scales as the bin size h is varied.

In terms of the mean value of δ_j for a given bin of size h, $\langle\delta\rangle$, we define $X(t)$ by

$$X\left(t\right) = \sum_{u=1}^{t} \left(\delta_u - \langle\delta\rangle\right). \tag{6}$$

The range R for the bin under consideration is defined as $Max(X(t)) - Min(X(t))$ where the maximum and minimum are taken for t between 1 and h. S denotes the standard deviation of the δ_j for the chosen bin.

In general the dimensionless rescaled range R/S varies with h for large h according to the scaling law [16,17]

$$\left(R/S\right) = \left(ch\right)^{\alpha}, \tag{7}$$

where α is the Hurst exponent. One can use linear regression analysis on a log-log plot of R/S against h to estimate the Hurst exponent α as the best fit slope of the log-log plot.

There are three types of generalized fractional Brownian motion:

- the persistent, for values of α in the range $0.5 < \alpha < 1$,
- the case $\alpha = 0.5$ is ordinary Brownian motion, and
- the (anti-)persistent, for $0 < \alpha < 0.5$.

A persistent type of fractional Brownian motion implies that the increments' persistence is maintained over longer periods of time, depending on the excess of the Hurst exponent value over 0.5. If at some time in the past there was an increase, it is more likely that there will be an increase in the future. A decreasing trend in the past implies the likelihood of a decreasing trend in the future. In the (anti-)persistent range any increasing trend in the past makes a decreasing trend in the future more probable, and vice versa.

Figure 2 shows the rescaled range regression analysis for the prime numbers in the range 961748941 . . . 982451653. These constitue the fiftieth million set of prime numbers. The horizontal axis is the log of the bin size ($log_2(h)$), and the vertical axis is the log of the mean R/S ($log_2(R/S)$) for the given values of h. The slope of

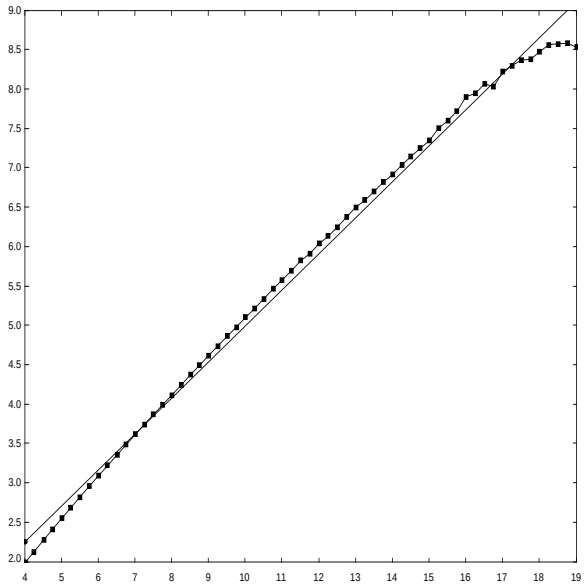

Fig. 2. Hurst exponent estimate for prime number differences for fiftieth million set of primes. The y axis is $log(R/S)$ and the x axis is the log of the bin size.

the best fit line gives the value of the Hurst exponent. The best fit line is also shown in the figure. The data is fairly linear. For lower values of h the scaling behaviour is not expected to hold, since it is an asymptotic phenomenon.

Table 3 presents the Hurst exponent for the twenty-fifth million and the fiftieth million primes. The number of zero differences used in the analysis was one million. The Hurst exponent is slightly below 0.5. Though the difference is small, it may be interesting given the evidence for a correlation between neighbouring prime numbers.

Table 1. Correlation between neighbouring primes, in the remainder on division by 6, for the fiftieth million and the tenth million set of primes.

Range of Primes	Remainder	1	5
961748941 ...	1	0.224	0.276
982451653	5	0.276	0.224
160481219 ...	1	0.222	0.278
179424673	5	0.278	0.222

Table 2. Correlation between neighbouring primes, in the remainder on division by 4, for the fiftieth million and the tenth million set of primes.

Range of Primes	Remainder	1	3
961748941 ...	1	0.226	0.274
982451653	3	0.274	0.226
160481219 ...	1	0.224	0.276
179424673	3	0.276	0.224

Table 3. Hurst exponent for distribution of prime numbers.

Range of Primes	Hurst exponent	Standard error
Twenty-fifth million	0.463	0.003
Fiftieth million	0.457	0.004

Table 4. Hurst exponent for degree 1 and degree 2 L-functions. r is an index to which of the group character representations is being considered.

Order of largest zero	Function	Hurst exponent	Fractal Dimension
	Riemann Zeta		
35161820		0.091	1.909
10^{12}		0.093	1.907
10^{21}		0.094	1.906
10^{22}		0.100	1.900
	Degree 1 L-function, Conductor 3		
31712310		0.092	1.908
	Degree 1 L-function, Conductor 4		
32457680		0.092	1.908
	Degree 1 L-function, Conductor 9		
	Dirichlet Character		
10000000	r=2 conjugate pair, negative roots	0.094	1.906
10000000	r=2 conjugate pair, positive roots	0.097	1.903
10000000	r=3 conjugate pair, negative roots	0.114	1.886
10000000	r=3 conjugate pair, positive roots	0.084	1.916
	Degree 1 L-function, Conductor 19		
	Dirichlet Character		
1000000	r=2 conjugate pair, negative roots	0.105	1.895
1000000	r=2 conjugate pair, positive roots	0.116	1.884
1000000	r=3 conjugate pair, negative roots	0.123	1.877
1000000	r=3 conjugate pair, positive roots	0.103	1.897
1000000	r=4 conjugate pair, negative roots	0.096	1.904
1000000	r=4 conjugate pair, positive roots	0.112	1.888
1000000	r=5 conjugate pair, negative roots	0.094	1.906
1000000	r=5 conjugate pair, positive roots	0.105	1.895
1000000	r=6 conjugate pair, negative roots	0.125	1.875
1000000	r=6 conjugate pair, positive roots	0.099	1.901
1000000	r=7 conjugate pair, negative roots	0.100	1.900
1000000	r=7 conjugate pair, positive roots	0.106	1.894
1000000	r=8 conjugate pair, negative roots	0.116	1.884
1000000	r=8 conjugate pair, positive roots	0.104	1.896
1000000	r=9 conjugate pair, negative roots	0.098	1.902
1000000	r=9 conjugate pair, positive roots	0.121	1.879
1000000	r=10 real representation	0.089	1.911
	Degree 2 Elliptic curve L-function Conductor 11 Isogeny class A		
100000		0.158	1.842
	Degree 2 Elliptic curve L-function Conductor 19 Isogeny class A		
100000		0.151	1.849
	Degree 2 L-function, Ramanujan tau associated cusp form weight 12, level 1		
284410		0.108	1.892

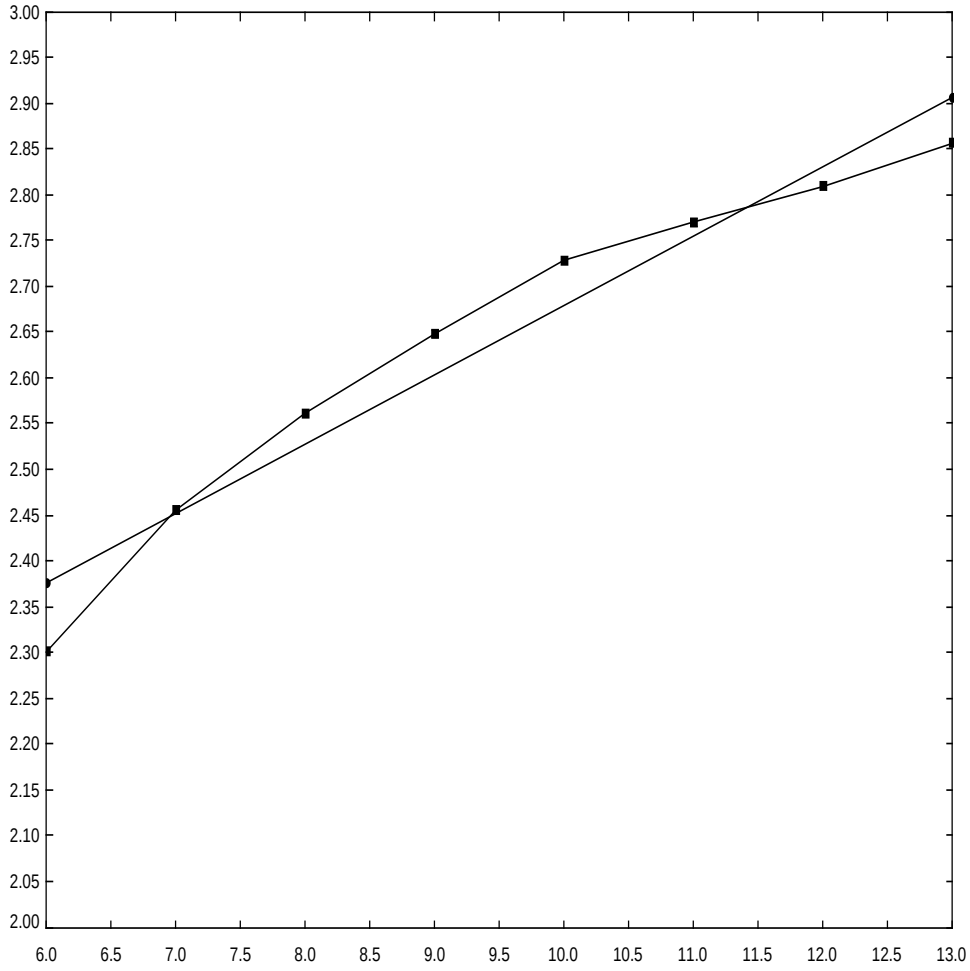

Fig. 3. Hurst exponent estimate for Riemann zeta zeros of height 10^{21}. The y axis is the base 2 log of the rescaled range and the x axis is the log of the bin size. The slope is 0.1

4. *L*-functions of degree 1 and degree 2

Given the interesting correlation observed in the distribution of prime numbers, and the relation of the distribution to the zeros of the Riemann zeta function and related L-functions, we now study these functions. Figure 3 is the rescaled range plot for Riemann zeta zeros of height 10^{21}, which gives a Hurst exponent of 0.1. Contrasting Figure 3 with Figure 2 highlights the unusual nature of the results for the L-functions.

The Riemann Zeta function is defined for $\mathrm{Re}(s) > 1$ by

$$\zeta(s) = \sum_{n=1}^{\infty} n^{-s} = \prod_{p} \left(1 - p^{-s}\right)^{-1}. \tag{8}$$

The product expression over the primes was first given by Euler. Eq. (8) converges for $\mathrm{Re}(s) > 1$. It was shown by Riemann [18,19,20,21] that $\zeta(s)$ has a continuation to the complex plane and satisfies a functional equation

$$\xi(s) := \pi^{-s/2}\,\Gamma(s/2)\,\zeta(s) = \xi(1-s); \tag{9}$$

$\xi(s)$ is entire except for simple poles at $s = 0$ and 1. The zeros of the Riemann zeta function are related to the distribution of prime numbers.

The remarkable properties of the Riemann Zeta Function can be generalised to a host of other zeta and L-functions, the study of whose properties pervades analytic number theory [23]. The simplest of the generalisations are for the Dirichlet L-functions $L(s,\chi)$ defined as follows: $q \geq 1$ is an integer and χ is a primitive character of the Abelian group formed by all integers smaller than and relatively prime to q. χ is extended to all integer values by making it periodic, and $\chi(m) = 0$ if m and q have a common factor. Then

$$L(s,\chi) = \sum_{n=1}^{\infty} \chi(n) n^{-s} = \prod_{p} \left(1 - \chi(p) p^{-s}\right)^{-1}. \tag{10}$$

The analogue of the functional equation Eq. (9) is known for the generalised zeta functions, and they also seem to satisfy the generalised Riemann Hypothesis. q is called the conductor of the L-function. The Riemann zeta function and Dirichlet L-functions are the degree 1 L-functions. Degree 2 L-functions [22] are asociated with cusp forms, and we study in particular the zeros of the degree 2 L-function associated with Ramanujan's $\tau(n)$.

We write the zeroes of the functions as $1/2 + i\gamma$. The generalised Riemann Hypothesis asserts that γ is real for the non-trivial zeroes. We order the γs in increasing order, with

$$\ldots\ldots \gamma_{-1} < 0 < \gamma_1 \leq \gamma_2 \ldots. \tag{11}$$

Then for the Riemann zeta function $\gamma_j = -\gamma_{-j}$ for $j = 1, 2, \ldots$, and $\gamma_1, \gamma_2, \ldots$ are roughly $14.1347, 21.0220, \ldots$. For the Dirichlet L-functions associated with complex character pairs, the positive and negative roots are not symmetrical, but are related by complex conjugation to the zeros of the L-function with the conjugate character. We apply the rescaled range analysis to study the distribution of the spacings $\delta_j = \gamma_{j+1} - \gamma_j$. The application of rescaled range analysis to the Riemann zeta function gave a variation in the Hurst exponent from 0.09 to 0.1 for zeroes covering the range 10^7 to 10^{22}, for sample sizes of 10000 zeros. This shows that there is a significant amount of self-affinity in the distribution of the zeroes. The low value of the exponent is interesting. It implies that there is a large degree of anti-persistence.

Because of this rather striking result, we apply the analysis to other functions which satisfy the generalised Riemann hypothesis.

We analyse the zeros of the Dirichlet L-function of conductor 9 and 19, and the Ramanujan tau L-function. Table 4 presents the Hurst exponent for these functions. The number of zero differences used in the analysis varied from 1000 to 5000. As we see from the table, these functions also show the same low Hurst exponents that was noticed for the Riemann zeta function. It is interesting that all the functions we have studied which satisfy the generalised Riemann hypothesis show a large degree of self-affinity and a large anti-correlation as shown by the low Hurst exponent. All distributions seem to have a high fractal dimension, 1.9. In view of the deep role of L-functions, and the fact that many of the L-functions show the property of a large negative correlation in the zero differences, it seems important to study the phenomenon further. A promising avenue may be the hypothesised relation to the semi-classical theory of classically chaotic quantum systems [24,25,26,27] and the relation to the spectra of random matrix theories (RMT) [28,29,30,31].

5. Formula for number variance of zeros

Given the low value for the Hurst exponent for the L-functions, the question arises as to what conclusion we can draw. One possible explanation is that the zeros indeed represent a long range anti-correlation. However, one has to be careful in coming to that conclusion, since a low Hurst exponent is rather special [33]. A proper interpretation of the results is based on some properties of rescaled range analysis which we explained in Section 3.

In this section we study the Riemann zeta zeros as a typical example. We show that the explanation is related to the the slow rate of growth of the function $S(t)$ [32,21], defined by

$$S(t) := \pi^{-1}\, arg\, \zeta(\frac{1}{2} + it), \tag{12}$$

rather than to true long-range anti-correlation. We use the formulae for the number variance of the zeros [24,25,26,27]. Asymptotically, for the Riemann zeta function the mean number of zeros with height less than γ (the smoothed Riemann zeta staircase) is [21]

$$< \mathcal{N}_{\mathcal{R}}(\gamma) >= (\gamma/2\pi)(ln(\gamma/2\pi) - 1) - \frac{7}{8}. \tag{13}$$

The interesting aspect of Eq. 13 is that for zeros of large height γ, the log term varies very little, and the behaviour for reasonable sample sizes is essentially linear. From the discussion in Section 3, it follows that Eq. 13 does not contribute to the rescaled range analysis, and the Hurst exponent depends on the fluctuations of $\mathcal{N}_{\mathcal{R}}(\gamma)$ from the smooth approximation $< \mathcal{N}_{\mathcal{R}}(\gamma) >$ in Eq. 13. The fluctuating part of the Riemann staircase function can be written as [25]

$$\mathcal{N}_{R,osc}(\gamma) = \mathcal{N}_{\mathcal{R}}(\gamma) - < \mathcal{N}_{\mathcal{R}}(\gamma) >= -\frac{1}{\pi} lim_{\eta \to 0} Im \ln \zeta(\frac{1}{2} - i(\gamma + i\eta)). \tag{14}$$

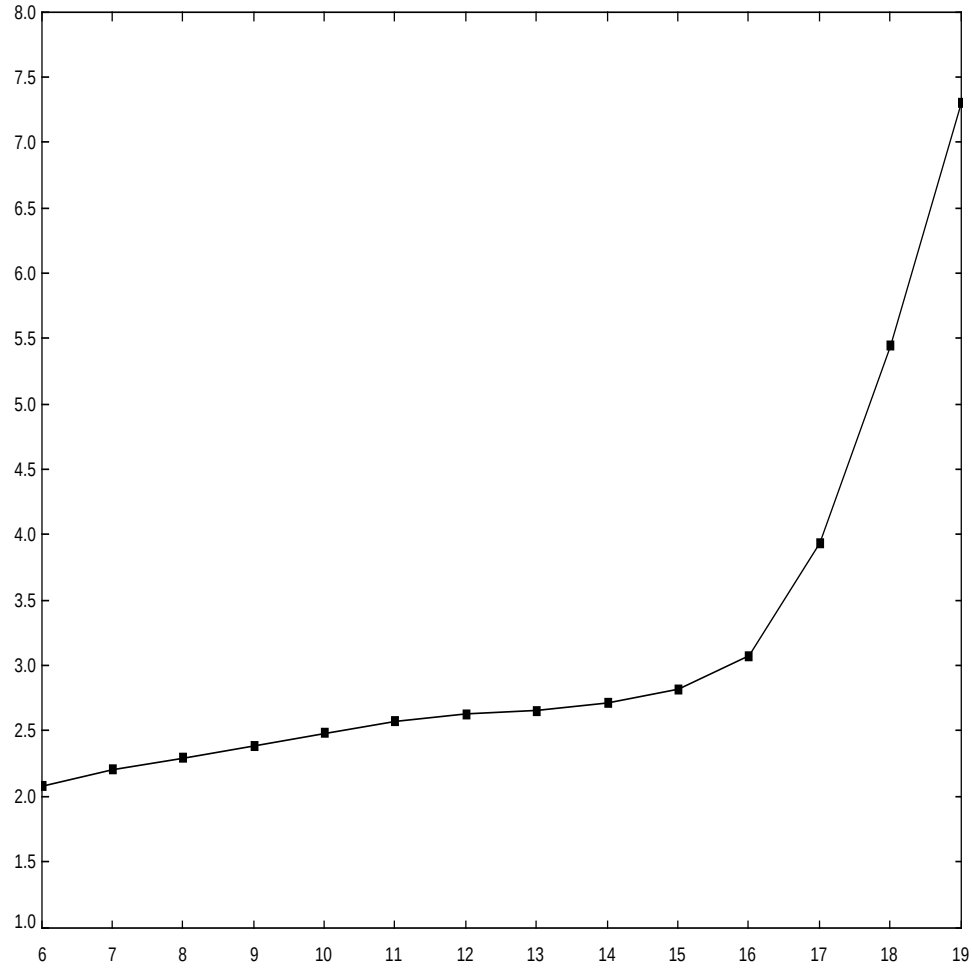

Fig. 4. Rescaled range analysis for Riemann zeta zeros of height 35161820. The y axis is the base 2 log of the rescaled range and the x axis is the log of the bin size.

The range of variation for this term is known to change very slowly with height γ, which accounts for the observed small value for the Hurst exponent.

In order to verify the explanation, we need to extend the sample size considered in the analysis so that the sample size is not too small compared to the height of the zeros. In Fig. 4 we show the result of the analysis for zeros of the Riemann zeta function of height 35161820. As can be seen from the figure, the effects of the non-linearity due to Eq. 13 raise the slope of the rescaled range curve when the sample size is not small compared to the height of the zeros. These considerations also predict that the range of zeros over which the low Hurst exponent is found increases with the height of the zeros. Thus, for the large height zeros the low

Hurst exponent will prevail for a very large range of zeros.

6. Conclusions

An analysis of the structure in the distribution of prime number gaps leads to the interesting result that the properties of a prime number are corelated with the properties of the preceeding prime number. A heuristic model has been presented to explain the correlation, and it has also been pointed out that further investigations are needed, particularly because the heuristic model does not explain the jumping champions phenomenon in the distribution of prime number gaps. The results for the L-functions are also interesting. All the functions we have studied which satisfy the generalised Riemann hypothesis show a large degree of self-affinity and a large anti-correlation as shown by the low Hurst exponent. All distributions seem to have a high fractal dimension, 1.9.

Appendix. Hermite Polynomials

Table 5. Hurst exponent for Hermite Polynomials.

order	Hurst exponent	Standard error
257	0.852	0.017
350	0.836	0.014

In this appendix, for completeness we briefly consider the rescaled range analysis for the zeros of the Hermite polynomials and Farey series. The local spacings of the zeroes of the Riemann Zeta function obey the laws for the (scaled) spacings between the eigenvalues of a typical large unitary matrix. That is, they obey the laws of the Gaussian Unitary Ensemble (GUE) [28,29,30,31]. The joint probability distributions [34] for the GUE eigenvalues for matrices of size N $\lambda_1 \geq \lambda_2 \ldots \geq \lambda_N$ is

$$2^{N(N-1)/2} exp\left(-\sum \lambda_i^2\right) \prod_{i<j} (\lambda_i - \lambda_j)^2 \; / \left(\pi^{N/2} \prod_{i=1}^{N} \Gamma(i)\right). \tag{A.1}$$

Edelman [34] shows that for large N the average characteristic polynomial approaches the Hermite polynomial of order N. Also, the set of eigenvalues λ_i which maximizes the joint probability distribution is given by the roots of the Hermite polynomial. We therefore consider the statistical properties of the roots of the Hermite polynomial.

Figure 5 shows the histogram of the zero differences for the Hermite polynomial of order 350. We observe that the histogram shows a sharp peak. There are no differences below a threshold value of 0.8. This is quite different from the distribution of differences for the eigenvalues of the GUE matrices.

The threshold for the zero differences can be understood in terms of the recursion

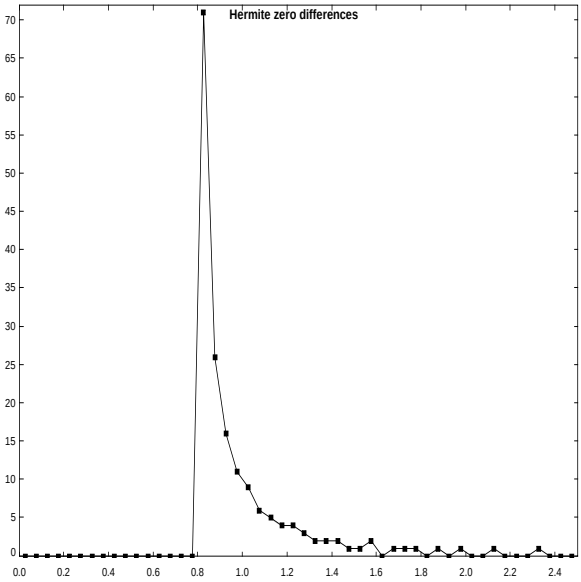

Fig. 5. Histogram of zero differences for Hermite polynomial of order 350. The y axis is the frequency and the x axis is the difference between neighbouring zeros.

relation for the Hermite polynomials. The recursion relation is

$$H_{n+1} = xH_n - \frac{n}{2}H_{n-1} \tag{A.2}$$

This implies that the zero of H_{n+1} is bounded from below by a zero of H_n, a property which holds for all the well-known orthogonal polynomials of mathematical physics. What is special to the Hermite polynomials is that the upper bound, which is normally the next zero of the lower order orthogonal polynomial, can be made stronger for Hermite polynomials. The upper bound is given by a zero of H_{n-1}. Thus, the bounds show that there the zeros of the Hermite polynomials are well-separated, accounting for the threshold in the histogram in Figure 5.

Table 5 presents the Hurst exponent for the Hermite polynomials of different order. The Hurst exponent is large, of order 0.8. The successive zero differences seem correlated positively.

Table 6. Hurst exponent for Farey Sequence.

order	Number of terms	Hurst exponent	Standard error
256	19949	0.432	0.003
512	79852	0.434	0.002
1025	319765	0.437	0.002
2048	1275587	0.440	0.002

The Farey sequence of order n is the sequence of completely reduced fractions between 0 and 1 which, when expressed in lowest terms, have denominators less than or equal to n, arranged in order of increasing size. Farey sequences can be used to give equivalent formulations of the Riemann hypothesis [21]. We apply rescaled range analysis to the Farey sequences of different order. Table 6 presents the Hurst exponent. The number of terms used in the analysis is also shown in the table. The Hurst exponent is slightly below 0.5. It is consistent with the successive differences not being correlated either positively or negatively.

References

1. Andrew Odlyzko, Michael Rubinstein and Marek Wolf, "Jumping Champions", *Experimental Mathematics*, **8**, 107-18, (1999).
2. Andrew Granville, "Prime Number Patterns", *American Mathematical Monthly*, **115**, 279-296, (2008).
3. E. Bombieri and H. Davenport: Small differences between prime numbers, *Proc. Royal Soc.* **A293** (1966), 1–18
4. R. P. Brent: The distribution of small gaps between succesive primes, *Math. Comp.* **28** (1974), 315–324.
5. R. P. Brent: Irregularities in the distribution of primes and twin primes, *Math. Comp.* **29** (1975), 43–56.
6. P. Erdos and E. G. Straus: Remarks on the differences between consecutive primes, *Elem. Math* **35** (1980), 115–118.
7. P. X. Gallagher: On the distribution of primes in short intervals, *Mathematika* **23** (1976), 4–9.
8. P. X. Gallagher: Corrigendum to distribution of primes in short intervals, *Mathematika* **28** (1981), 86.
9. H. Halberstam and H. -E. Richert: *Sieve Methods*, Academic Press 1974.
10. Chris K. Caldwell, Lists of small primes, *Technical Report* (2008), http://primes.utm.edu/lists/small/.
11. O. Shanker, Generalised Zeta Functions and Self-Similarity of Zero Distributions, *J. Phys. A* **39**(2006), 13983-13997.
12. H. E. Hurst, "Long term storage capacity in reservoirs," *Trans. Am. Soc. Civ. Eng*, **116** , 770-799, (1951).
13. W. Feller, "Introduction to Probability Theory and its Applications," John Wiley, (1966).
14. J. Feder, "Fractals," Plenum Press, (1991).
15. E. E. Peters, "Chaos and Order in the Capital Markets," John Wiley and Sons, Inc., (1991).
16. B.B. Mandelbrot, J. Van Ness, *SIAM Review*, **10** , 422-437, (1968).
17. B.B. Mandelbrot, "The Fractal Geometry of Nature," Freeman and Co., (1982).
18. B. Riemann, "Über die Anzahl der Primzahlen uter Einer Gegebenen Gröbe," *Montasb. der Berliner Akad.*, (1858), 671-680.
19. B. Riemann, "Gesammelte Werke", Teubner, Leipzig, (1892).
20. E. Titchmarsh, "The Theory of the Riemann Zeta Function," Oxford University Press, Second Edition, (1986).
21. H. M. Edwards, "Riemann's Zeta Function," Academic Press, (1974).
22. M. Rubinstein, *Evidence for a Spectral Interpretation of Zeros of L-functions*, PhD thesis, Princeton University, 1998.

23. Stephen S. Gelbart, Stephen D. Miller, "Riemann's Zeta Function and Beyond", *Bulletin of the AMS*, **41** , 59-112, (2003).
24. M. V. Berry, "Semiclassical theory of spectral rigidity," *Proc. R. Soc.*, **A 400** , 229-251, (1985).
25. M. V. Berry, "Riemann's zeta function: a model for quantum chaos?," *Quantum chaos and statistical nuclear physics (Springer Lecture Notes in Physics)*, **263** , 1-17, (1986).
26. M. V. Berry, "Quantum Chaology," *Proc. R. Soc.* , **A 413** , 183-198, (1987).
27. M. V. Berry, 'Number variance of the Riemann zeros',' *NonLinearity* , **1** ,399-407 , (1988).
28. E. Wigner, "Random Matrices in Physics," *Siam Review*, **9**, 1-23, (1967).
29. M. Gaudin, M. Mehta, "On the Density of Eigenvalues of a Random Matrix," *Nucl. Phys.*, **18**, 420-427, (1960).
30. M. Gaudin, "Sur la loi Limite de L'espacement de Valuers Propres D'une Matrics Aleatiore," *Nucl. Phys.*, **25**, 447-458, (1961).
31. F. Dyson, "Statistical Theory of Energy Levels III," *J. Math. Phys.*, **3**, 166-175, (1962).
32. A. Odlyzko, "The 10^{20}-th Zero of the Riemann Zeta Function and 70 Million of its Neighbors," (preprint), A.T.T., (1989).
33. Govind Rangarajan and Mingzhou Ding, "An Integrated Approach to the Assessment of Long Range Correlation in Time Series Data", *Phys. Rev.*, **E61**, 4991-5001, (2000).
34. A. Edelman, *Eigenvalues and Condition Numbers of Random Matrices*, PhD thesis, Massachusetts Insititute of Technology, 1989.